ACS APPLIED MATERIALS & INTERFACES

www.acsami.org

Research Article

Fouling and Retention Mechanisms of Selected Cationic and Anionic Dyes in a $Ti_3C_2T_x$ MXene-Ultrafiltration Hybrid System

Sewoon Kim, Miao Yu, and Yeomin Yoon*

Cite This: *ACS Appl. Mater. Interfaces* 2020, 12, 16557–16565

Read Online

ACCESS | Metrics & More | Article Recommendations | Supporting Information

ABSTRACT: $Ti_3C_2T_x$ MXenes, a very new family of nanostructured material, were applied in combination with an ultrafiltration (UF) membrane (MXene-UF) for removal of the selected dyes including methylene blue (MB) and methyl orange (MO) as the first attempt. The normalized flux of the MXene-UF (0.90 for MB and 0.92 for MO) indicated better performance than a single UF (0.86 for MB and 0.90 for MO) and a powdered activated carbon (PAC)-UF (0.72 for MB and 0.75 for MO) for both dyes. The addition of an adsorbent decreased the irreversible fouling of the hybrid system compared to single UF, due to adsorption of dyes. The observed dominant fouling mechanism was cake layer fouling, evaluated using a resistance-in-series model, permeate flux modeling, and four conceptual blocking law models. PAC in particular acted as a foulant, leading to a severe flux decline. The average retention rate was found to be on the order of PAC-UF (57.7 and 47.9%) > MXene-UF (51.7 and 34.9%) > single UF (45.0 and 34.7%) for MB and MO, respectively. The results showed that although PAC exhibits relatively strong adsorption performance, MXene-UF also exhibited high selectivity due to electrostatic interaction between the MXene and dyes. In addition, humic acid (HA) adsorption on the membrane led to a reduction in the effective membrane area, resulting in a higher retention and lower flux for MXene-UF in the presence of HA. Furthermore, higher retention was observed for MXene-UF at pH 10.5 compared to pH 3.5 and 7, because MXene has more negative terminations at higher pH, leading to greater MB adsorption. Additionally, because of the bridging effect between the membrane and the MXene and competition between MB and cation ions for adsorption on the MXene, lower retention and flux were observed in MXene-UF with background ions.

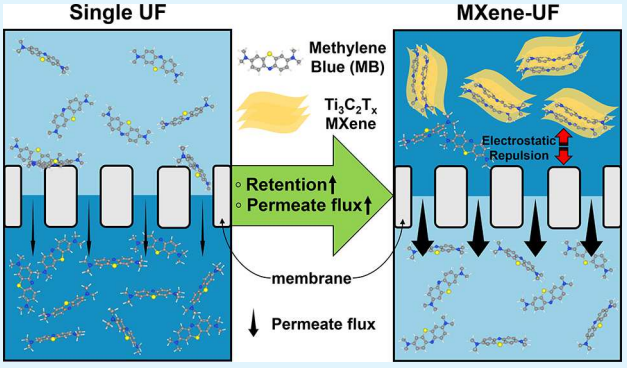

KEYWORDS: *membrane, adsorption, MXene, dyes, fouling mechanism, removal mechanism*

1. INTRODUCTION

Population growth and industrial development have led to a wide range of organic contaminants being discharged into the environment. In particular, dyes released from the textile, paper, leather, plastics, and food industries have been found in increasing concentrations in water streams.[1] Due to their toxicity and high oxygen demand, residual dyes in water sources can have significant adverse effects on human life and ecosystems, even at low concentrations. In addition, conventional water and/or wastewater treatment systems cannot always reduce dye concentrations to acceptable levels because of their stability and complexity.[2] A number of water treatment technologies have been proposed to treat dyes. Among these, membrane processes have gained in popularity because of their ease of operation, low physical space requirements, and high separation efficiency.[3] However, although membrane processes can effectively treat dyes in water, these compounds can also act as foulants, leading to decreased flux performance. In addition, membrane-based technologies involving nanofiltration (NF) and reverse osmosis (RO) have a relatively high operating cost.[4] The enhancement of productive strategies for fouling control and an economical membrane system is necessary.

To resolve the drawbacks of a conventional membrane system, an abundance of study is suggested including membrane surface modification,[5] a multistage membrane process,[6] micellar-enhanced ultrafiltration (UF),[7] and so on. Inter alia, combining adsorption with an UF hybrid system using commercialized powdered activated carbon (PAC) as an adsorbent (termed a "PAC-UF" in this paper) has received attention for control of organic contaminants.[8] Adsorption has been shown to improve the retention rate of UF when used as a pretreatment.[9] The UF process, acting as a low-pressure membrane, is relatively cost-effective compared to NF and RO, and provides effective separation, including of used PAC from

Received: February 8, 2020
Accepted: March 17, 2020
Published: March 17, 2020

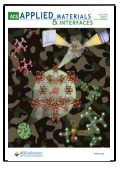

https://dx.doi.org/10.1021/acsami.0c02454
ACS Appl. Mater. Interfaces 2020, 12, 16557–16565

feedwater. Nevertheless, some studies have reported that PAC can have a negative effect on permeate flux,[10] and work has been undertaken to develop better adsorbents for improved performance, including both retention and permeate flux.

MXenes are a relatively new family of multilayered two-dimensional transition metal carbides, which have been evaluated for use in a number of applications including energy storage, transparent conductive electrodes, and water purification.[11,12] In particular, some studies have demonstrated that a range of pollutants for water treatment are effectively removed by MXenes used as adsorbents because of their excellent stability, superior oxidation resistance, fine structure, and high electrical/metallic conductivity.[13,14] For example, Peng et al. reported 95% lead (C_0 = 50 mg/L) removal efficiency using 0.025 g/50 mL of MXene.[15] Wang et al.[14] and Meng et al.[16] reported 95% Re(VII) (C_0 = 10 mg/L) and 80% urea (C_0 = 30 mg/L) removal with 8 mg/20 mL and 0.155 g/6 mL of MXene, respectively. Another study indicated that 100 mg/100 mL of MXene resulted in 40% methylene blue (MB) removal (C_0 = 0.05 mg/mL).[17] While these reports indicate that MXenes are attractive materials for removal of contaminants in water treatment processes, most studies have focused on the use of MXene in adsorption processes. In addition, although these studies demonstrated high removal rates, the MXene dosages were unrealistically high for use in a real water treatment plant.[18] Therefore, there is still a requirement for study into the various applications of MXene in real water treatment systems, such as the potential for combining MXene with a UF hybrid system (termed "MXene-UF" in this paper). Particularly, there have been no performance studies on the effect of MXene as a foulant in UF.

In this work, MXene-UF is applied for the removal of dyes from water in one attempt. Scanning electron microscopy and transmission electron microscopy (SEM and TEM, respectively), X-ray diffractometry (XRD), and surface area and pore size analysis were employed to investigate the textural characteristics of the MXene. Synthetic dye containing wastewater as a feed solution was used to briefly determine the feasible performance of single UF, MXene-UF, and PAC-UF. MB and methyl orange (MO) were employed to represent commonly used cationic and anionic dyes. Permeate flux and retention variation were observed as a function of the volume concentration factor (VCF) in a single UF and both hybrid systems. In addition, in the hybrid systems, the role played by the MXene and PAC in fouling was studied via a resistance-in-series model, permeate flux modeling, and four conceptual blocking law models. Finally, for better understanding of its application in a real water treatment system, MXene-UF was evaluated under a range of conditions with various concentrations of natural organic matter (NOM), pH, and background ions with regard to permeate flux and retention rate.

2. EXPERIMENTAL SECTION

2.1. Materials. Two different adsorbents were used for adsorbent-UF: MXene and PAC. $Ti_3C_2T_x$ MXene was purchased from the Advanced Materials Development Expert Store (Hangzhou, Zhejiang, China). Commercially available PAC was obtained from Evoque Water Technologies (Randolph, MA, USA). MB and MO, as target dye compounds, were purchased from Sigma-Aldrich (St. Louis, MO, USA). The concentration of these compounds was determined using a UV−vis spectrophotometer (Agilent Technologies, Santa Clara, CA, USA) based on absorbance at 464 and 665 nm, respectively. A commercial flat sheet polyamide membrane was acquired from GE Osmonics Inc. (Minnetonka, MN, USA). The physicochemical properties of the target compounds and membrane are summarized in Tables S1 and S2, respectively. To evaluate the effect of a range of water conditions on the treatment system, humic acid (HA) was used as the most dissolved NOM compound, HCl and NaOH were used to evaluate the effect of pH, and NaCl, $CaCl_2$, and Na_2SO_4 were used to investigate the effect of background ions (all purchased from Sigma-Aldrich).

2.2. Characterizations. The physicochemical properties of the MXene were analyzed using several instruments, as shown in Figure S1. SEM (S-4200; Hitachi, Tokyo, Japan) and TEM (Titan G2; FEI, Hillsboro, OR, USA) were used for surface morphology characterization, and the structure of the MXene was confirmed by XRD (D/max-2500; Rigaku, Tokyo, Japan). Surface charge was measured using a zeta potential analyzer (ZetaPals; Brookhaven Instruments Corporation, Holtsville, NY, USA). Finally, a Micromeritics ASAP 2020 static volumetric adsorption unit (Micromeritics Inc., Norcross, GA, USA) was used to obtain nitrogen adsorption and desorption equilibrium data at −196 °C. The surface area of the MXene was estimated based on these data using Brunauer−Emmett−Teller (BET) models.

2.3. Operation and Evaluation of MXene-UF. The performance of the membrane systems was investigated by dead-end cell filtration (Sterlitech Co., Kent, WA, USA) with an effective membrane area of 14.6 cm^2 and a total feed volume of 300 mL. The membrane was washed gently with deionized (DI) water and then stored in DI water at 4 °C before use. Only membranes exhibiting ≤10% permeability variation in a pure water permeability (PWP) test were used in this study. As the pretreatment, adsorption was performed with 2 mg/L of the selected dye and 20 mg/L of adsorbent for 2 h at 200 rpm. Generally, 5−50 mg/L of adsorbent and a contact time of 1−5 h are used in water treatment plants.[19] Membrane filtration was then conducted at a transmembrane pressure of 75 psi (520 kPa), with a stirring speed of 200 rpm. To evaluate the retention rate of the selected dyes and the permeate flux, 20 mL amounts of each permeate sample were collected until 60 mL of retentate and 240 mL of permeate were obtained, corresponding to 1.1−5 of VCF. The VCF, retention rate, and permeate flux were calculated using eqs (S1), (S2), and (S3), respectively.

The transportation mechanism of the selected dye compounds in the single UF, MXene-UF, and PAC-UF systems was evaluated via resistance-in-series, flux modeling, and four conceptual blocking law models. Darcy's law is commonly used to describe the permeate flux (J) for membrane filtration[20]

$$J = \frac{\Delta P}{\eta(R_m + R_f)} = \frac{\Delta P}{\eta(R_m + R_{re} + R_{irr})} = \frac{\Delta P}{\eta(R_m + R_c + R_{ad})} \quad (1)$$

where J is the water flux through a membrane (L/m^2/h), ΔP is the pressure drop through the membrane (kPa), η is the dynamic viscosity of the fluid (kg/m/s), and R_m is the hydrodynamic resistance of the membrane (1/m). Also, during membrane filtration, membrane fouling (R_f) affects the total resistance to flow. A number of factors contribute to R_f, including cake resistance resulting from the accumulation of feed on the membrane surface (R_c, 1/m) and adsorption (R_{ad}, 1/m), consistent with reversible resistance (R_{re}, 1/m) and irreversible resistance (R_{irr}, 1/m). Eq 1 was used to calculate the effects of these different resistance types.[20]

The cake filtration model represents one method for evaluating the fouling mechanism. This model is widely applied to assess the membrane filtration index (MFI) under constant pressure filtration. The MFI is determined as the second linear slope line obtained from plotting t/V against V.[20,21]

$$\frac{t}{V} = \frac{\eta R_m}{A\Delta P}t + \frac{\eta \alpha C_f}{2\Delta P}V = = \frac{\eta R_m}{A\Delta P}t + \mathrm{MFI}\cdot V \quad (2)$$

where t is the filtration time (h), V is the permeate volume (m^3), A is the effective membrane area (m^2), C_f is the dye concentration in the feed (mg/L), and α is the specific cake resistance for each cake layer

https://dx.doi.org/10.1021/acsami.0c02454
ACS Appl. Mater. Interfaces 2020, 12, 16557−16565

(m/g). Permeate flux modeling can also be used to calculate the MFI as a quarter of the β constant in eq 3, which can be simply expressed in the form $J^2 = (\alpha + \beta t)^{-1}$.[22]

$$J^2 = \left[\left(\frac{\eta R_m}{\Delta P}\right)^2 + \left(\frac{2\eta\alpha C_f}{\Delta P}\right)t\right]^{-1} \quad (3)$$

The model constants α and β were obtained using SigmaPlot 12.3 software (Systat Software, Inc., San Jose, CA, USA) to allow performance of a nonlinear regression analysis.

Finally, four conceptual blocking law models incorporating specific operating conditions, including constant pressure, a cylindrical membrane pore, and non-Newtonian fluids were used to explain the fouling mechanisms, as shown in eq 4.[23,24]

$$\frac{d^2t}{dV^2} = k\left(\frac{dt}{dV}\right)^n \quad (4)$$

where n is the blocking index, set at 2, 1.5, 1, and 0 for complete blocking, standard blocking, intermediate blocking, and cake filtration, respectively.

3. RESULTS AND DISCUSSION

3.1. Characterization of the MXene. The morphology of the MXene, which is a multilayered two-dimensional material, can be seen in the SEM image in Figure S1a. The TEM micrograph (Figure S1b,c) clearly also indicated that the MXene was multilayered, with a gap thickness from 0.92−0.95 nm, similar to the results obtained in a previous study.[25] Furthermore, the XRD pattern for the MXene, shown in Figure S1d, is consistent with previously reported studies, indicating successful synthesis of the MXene.[26,27] The material surface charge density can be estimated from the zeta potential value. The point of zero charge (PZC) of the MXene was measured at pH 3 based on the zeta potential value, as shown in Figure S1e. This is presumably because the T_x, which represent surface termination units in $Ti_3C_2T_x$ MXene, is −OH, −O, and/or −F.[11] Also, the PZC of the membrane was shown at pH 3 in Figure S2. These PZC values indicate that both MXene and the membrane negatively charged under neutral pH can actively adsorb positively charged compounds through electrostatic attraction, while those may have small adsorption with negatively charged compounds due to electrostatic repulsion. Finally, the BET surface area of the MXene was estimated from the equilibrium data of adsorption and desorption of nitrogen at −196 °C. Figure S1f shows the 9 m^2/g MXene surface area; this value is similar to that reported earlier.[28] Therefore, the SEM, TEM, XRD, zeta potential analysis, and surface area results indicate that MXene has potential for use in adsorbent-UF for removal of the selected dyes.

To confirm the feasibility of MXene-UF to remove dye compounds, Figure 1 presents that retention rate and normalized flux in single UF, MXene-UF, and PAC-UF with synthetic dye wastewater as a feed solution. Also, the composition of synthetic dye wastewater was described in Table S3. While 65.4% of the dye retention rate in single UF was achieved, significantly higher retention rates in the presence of 20, 50, and 100 mg/L of each adsorbent were observed; 80.2, 90.7, and 99.1% for MXene-UF and 85.5, 91.7, and 99.5% for PAC-UF, respectively. Also, although a similar normalized flux was shown with an increasing MXene dose (0.90 for 20 mg/L, 0.89 for 50 mg/L, and 0.89 for 100 mg/L) compared to single UF (0.90), significant flux decline was observed in PAC-UF with increasing PAC dose (0.79 for 20 mg/L, 0.72 for 50 mg/L, and 0.60 for 100 mg/L). These results indicate that MXene-UF can be applied to treat dye containing wastewater with a high retention rate and less flux decline. Meanwhile, mechanism evaluation for retention and fouling is very important to understand performance. Thus, the effect of each composition for detailed performance was evaluated by the following studies.

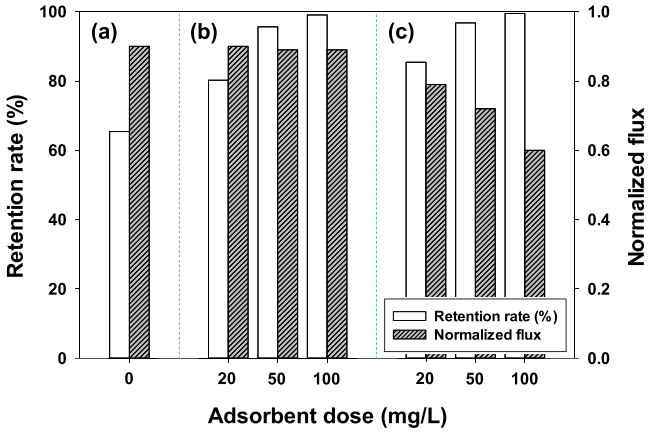

Figure 1. Retention and normalized flux variation for synthetic dye wastewater in (a) single UF, (b) MXene-UF, and (c) PAC-UF. Operating conditions: VCF = 1.25 (recovery = 20%), ΔP = 75 psi (520 kPa), precontact time = 2 h, and stirring speed = 200 rpm.

3.2. Flux Decline in Hybrid System. The declining flux behaviors of the selected dyes in the single UF, MXene-UF, and PAC-UF treatments are shown as a function of VCF in Figure 2. The normalized fluxes of MB and MO in single UF at VCF = 5 decreased gradually, to 0.86 and 0.90, respectively. A slightly higher normalized flux was observed in MXene-UF (0.90 for MB and 0.92 for MO at VCF = 5) than in single UF. In contrast, a rapid flux decline was observed for MB and MO in PAC-UF, with values of 0.72 and 0.75, respectively, at VCF = 5. These results show that MB had a greater impact on the flux decline than MO. Both compounds have a similar molecular weight (319.85 g/mol for MB and 327.33 g/mol for MO); however, positively charged MB can be more readily deposited on the negatively charged membrane at pH 7 compared to negatively charged MO, resulting in a decreasing

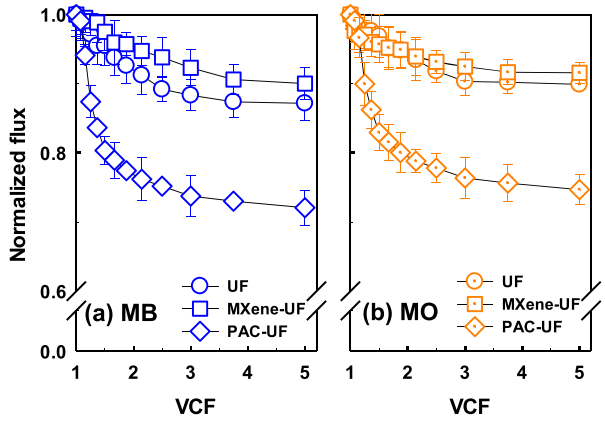

Figure 2. Normalized flux variation as a function of VCF for (a) MB and (b) MO. Operating conditions: ΔP = 75 psi (520 kPa), adsorbent = 20 mg/L, dye = 2 mg/L, pH = 7, conductivity = 100 μS/cm, precontact time = 2 h, and stirring speed = 200 rpm.

https://dx.doi.org/10.1021/acsami.0c02454
ACS Appl. Mater. Interfaces 2020, 12, 16557−16565

membrane surface and pore size.[29,30] In addition, an enhanced membrane flux was observed in MXene-UF compared to single UF, while deterioration of the permeate flux was observed in PAC-UF. This is presumably because, while some MXene with OH and/or O terminations can interact with COOH, NHCO, and NH_2 in a polyamide membrane by forming hydrogen bonds,[31,32] most MXenes with negative charge (estimated based on zeta potential value; Figure S1e) cannot easily attach onto the membrane due to electrostatic repulsion. In contrast, PAC has more functional groups, higher hydrophobicity, and less negatively characteristics compared to MXene, so flux decline can arise through PAC deposition on the membrane.[19,33]

Comprehensive understanding of fouling resistance is essential for improving the performance of this hybrid system. Therefore, evaluation of fouling phenomena was conducted using a resistance-in-series model, as shown in Table 1. The

Table 1. Fouling Resistances, Specific Cake Resistances (ε), and Specific Adsorption Resistances (δ) for Selected Dyes in the Single UF, MXene-UF, and PAC-UF Systems

	MB			MO		
	UF	MXene-UF	PAC-UF	UF	MXene-UF	PAC-UF
R_t ($\times 10^{12}$ m^{-1})	88.8	85.0	106	85.4	83.9	102
R_m ($\times 10^{12}$ m^{-1})	76.5	76.5	76.5	76.8	769	76.2
R_c ($\times 10^{12}$ m^{-1})	7.99	4.76	25.3	5.91	5.43	22.4
R_{ad} ($\times 10^{12}$ m^{-1})	4.28	3.72	4.31	2.70	1.63	3.44
R_c/R_t	0.09	0.06	0.24	0.07	0.06	0.22
R_{ad}/R_t	0.05	0.04	0.04	0.03	0.02	0.03
ε ($\times 10^{12}$ m/g)	22.7	13.8	76.5	14.7	13.8	59.9
δ ($\times 10^{12}$ m/g)	12.1	10.8	13.0	6.72	4.13	9.21

overall filtration resistance (R_t) with MB (88.8 for single UF, 85.0 for MXene-UF, and 106 for PAC-UF) was higher than for MO (85.4 for single UF, 83.9 for MXene-UF, and 102 for PAC-UF), indicating that a relatively larger flux decline was generated with MB. A higher value for both cake formation resistance (R_c) (7.99 for single UF, 4.76 for MXene-UF, and 25.3 for PAC-UF) and adsorptive fouling resistance (R_{ad}) (4.28 for single UF, 3.72 for MXene-UF, and 4.31 for PAC-UF) was obtained with MB compared to MO, for all three systems (R_c: 5.91 for single UF, 5.43 for MXene-UF, and 22.4 for PAC-UF, R_{ad}: 2.70 for single UF, 1.63 for MXene-UF, and 3.44 for PAC-UF). These results support the conclusion that MB can be more easily deposited on both the surface of, and inside, the membrane by electrostatic attraction. In addition, the value of R_c/R_t for MB and MO in MXene-UF was the same, at 0.06, while R_{ad}/R_t for MB (0.04) was higher than that for MO (0.02). This also indicates that MO can generate a relatively lower adsorptive fouling due to electrostatic repulsion. Furthermore, MXene was a positive influence on both the R_c and R_{ad} values in filtration compared to single UF, which indicates that electrostatic repulsion rather than hydrogen bonding occurs between MXene and the membrane. However, the highest R_t, R_c, and R_{ad} values were observed for PAC-UF compared to single UF and MXene-UF, demonstrating that PAC acts as a foulant by adsorbing and depositing on the membrane.

To quantify the reversible and irreversible fouling potential of the three different systems, the total cake formation resistance per mass of the retained selected dyes and/or adsorbent (specific cake resistance, ε) and the total adsorptive resistance per mass of the retained selected dyes and/or adsorbent (specific adsorptive resistance, δ) were evaluated.[34] A number of previous studies have suggested that cake formation resistance caused by the deposition of foulants is generally reversible.[35] In contrast, the internal pore fouling resistance of the membrane due to the adsorption of foulants is often irreversible.[36] Both the ε and δ values of single UF (ε: 22.7, δ: 12.1 for MB, ε: 14.7, δ: 6.72 for MO) were higher than for MXene-UF (ε: 13.8, δ: 10.8 for MB, ε: 13.8, δ: 4.13 for MO) and lower than for PAC-UF (ε: 53.1, δ: 36.4 for MB, ε: 37.5, δ: 31.6 for MO). These observations indicate that the amount of dye and/or adsorbent, as a potential cause of both cake formation and adsorptive resistance in single UF, was higher than in MXene-UF and lower than in PAC-UF. In other words, MXene can enhance the ε and δ values by adsorbing dyes and not depositing excessively on the membrane. However, although PAC can adsorb the selected dyes, additional deposition occurs with PAC acting as a foulant. The ε value was higher than the δ value under all experiment conditions, indicating that reversible fouling dominates over irreversible fouling. Therefore, MXene-UF is superior to single UF and PAC-UF in terms of flux decline, due to dye adsorption by MXene and low deposition of MXene on the membrane because of electrostatic repulsion.

3.3. Fouling Mechanisms in Hybrid System. To analyze the flux decline of MB and MO in detail, permeate flux modeling was performed for single UF, MXene-UF, and PAC-UF, as shown in Figure S3. Permeate flux modeling (J^2 vs time) based on experimental flux data is widely used to evaluate model constants (α and β) and MFI values in linear form.[37] In particular, the MFI value, which is based on the cake filtration fouling mechanism, is needed to obtain the fouling potential and mitigate flux decline.[38,39] The model constants and MFI values are presented in Table 2. Less cake formation

Table 2. Analyses of Permeate Flux Modeling for MB and MO in the Single UF, MXene-UF, and PAC-UF Systems

		α (min^2/m^2)	β (min/m^2)	r^2	MFI (min/m^2)
MB	UF	1915	341	0.9275	85.2
	MXene-UF	1880	262	0.9270	65.5
	PAC-UF	1849	919	0.9293	230
MO	UF	1762	186	0.9227	46.6
	MXene-UF	1726	123	0.9209	30.8
	PAC-UF	1834	711	0.9296	178

is observed for MXene-UF compared to single UF, as stated previously, leading to a lower MFI value. This result supports the conclusion that the MXene has a positive effect on flux decline due to electrostatic repulsion with the membrane. In contrast, it was found in the previous section that PAC, as a foulant, had a negative effect on the permeate flux through deposition on the membrane. This can also be seen in the higher MFI value for PAC-UF, because the MFI value is proportional to the extent of cake formation. This finding indicates that PAC can more easily form a cake layer than the MXene, consistent with the result of the resistance-in-series model.

Four conceptual blocking models, which have been widely used to evaluate membrane fouling at constant transmembrane pressure, were generated to describe the fouling mechanism

https://dx.doi.org/10.1021/acsami.0c02454
ACS Appl. Mater. Interfaces 2020, 12, 16557−16565

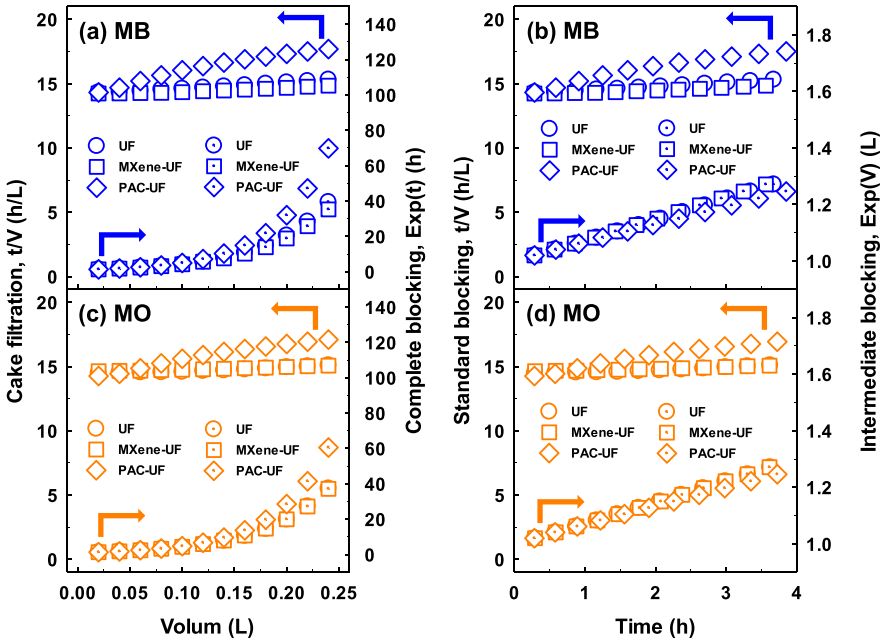

Figure 3. Four conceptual blocking law models at 75 psi (520 kPa) in the single UF, MXene-UF, and PAC-UF systems. (a) Cake filtration and complete blocking analysis for MB, (b) standard blocking and intermediate blocking analysis for MB, (c) cake filtration and complete blocking analysis for MO, and (d) standard blocking and intermediate blocking analysis for MO.

(Figure 3).[37,40] The r^2 values obtained by linear regression on each fouling mechanism are summarized in Table S4. It appears that, although the value for cake filtration (r^2: 0.9959 for MB and 0.9584 for MO) was slightly higher than that for standard blocking (r^2: 0.9951 for MB and 0.9519 for MO) for both dyes in single UF, both fouling mechanisms had relatively higher values than complete (r^2: 0.9009 for MB and 0.9040 for MO) and intermediate blocking (r^2: 0.9006 for MB and 0.9019 for MO). This is presumably because cake filtration is caused by the accumulation of dyes in the cake layer. In addition, because both MB and MO have a size of about ∼20 Å, which is smaller than the membrane pore (26−30 Å), some part of each dye can be adsorbed by hydrogen bonding into the membrane pore walls.[41] Cake filtration (r^2: 0.9690) for MB in MXene-UF showed better fitting results compared to complete (r^2: 0.9089), standard (r^2: 0.9434), and intermediate blocking (r^2: 0.9053), whereas cake filtration (r^2: 0.9876) and standard blocking (r^2: 0.9854) showed slightly higher values than complete (r^2: 0.9809) and intermediate blocking (r^2: 0.9794) for MO in MXene-UF. This indicates that MB can be adsorbed on MXene by electrostatic attraction, resulting in reduced internal membrane fouling.[17,26] Cake filtration showed the best fitting results for both dyes in PAC-UF, due to deposition of PAC on the membrane surface. Also, the n value was used for determining the fouling mechanism from d^2t/dV^2 versus dt/dV as shown in Figure S4. The n values under all conducted systems were shown to be approximately 0, which confirms that cake filtration is dominant and corresponds with the results of four conceptual blocking models.[42] Therefore, flux decline caused by reversible fouling, i.e., a cake layer, is the dominant fouling mechanism for removal of the selected dyes in all three systems. In addition, both hybrid systems exhibited reduced irreversible fouling compared to single UF, due to the addition of the adsorbent during filtration.

3.4. Retention and Mechanisms in the Hybrid System. Figure 4 shows the retention performance of MB and MO at pH 7, as a function of the VCF, in single UF, MXene-UF, and PAC-UF. The average retention rate in single UF was about 45.0% for MB and 34.7% for MO. This is because both dyes can interact with the membrane. Hydrogen bonding can occur between polyamide membranes with COOH, NHCO, and NH_2 and dyes with N and O.[43] Also, hydrophobic interaction can occur between the aromatic rings of the membrane and those of MB and MO.[2,44] Furthermore, electrostatic interaction between the membrane and dyes can affect the retention rate, because MB contains positively charged nitrogen, and MO has a negatively charged sulfonate group.[45] A higher retention rate was observed for MB compared to MO in single-UF, because MB is hydrophobic and hence has a higher octanol−water distribution coefficient (log D_{OW}: 2.60) than MO (log D_{OW}: 1.29) at pH 7. Additionally, electrostatic attraction between MB and a negatively charged membrane can enhance the retention rate through deposition on the membrane. In contrast, some part of MO can be retained on the feed side due to electrostatic repulsion with the membrane, which prevents the dye from passing through. Nevertheless, the higher retention of MB in

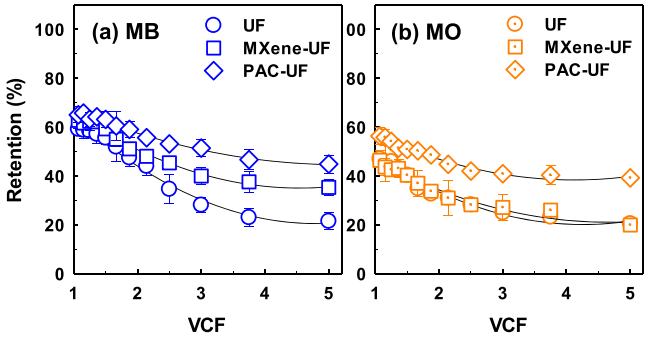

Figure 4. Retention variation as a function of VCF for (a) MB and (b) MO. Operating conditions: ΔP = 75 psi (520 kPa), adsorbent = 20 mg/L, dye = 2 mg/L, pH = 7, conductivity = 100 μS/cm, precontact time = 2 h, and stirring speed = 200 rpm.

https://dx.doi.org/10.1021/acsami.0c02454
ACS Appl. Mater. Interfaces 2020, 12, 16557−16565

single UF indicates that both hydrophobic interaction and electrostatic attraction dominate. Furthermore, removal efficiencies increased with adsorbent in both hybrid systems. PAC-UF exhibited better average retention rates, of 57.7% for MB and 47.9% for MO, compared to MXene-UF (51.7% for MB and 34.9% for MO). It was previously mentioned that both hydrogen bonds and electrostatic interaction exist between the MXene and both dyes in MXene-UF.[16] However, PAC can more easily reduce the membrane surface and pore size than MXene by depositing on the membrane, resulting in a higher retention rate. Also, both dyes can be more easily adsorbed on PAC than on MXene because of the higher surface area and increased hydrophobic interaction, hydrogen bonding, and electrostatic interaction. Thus, PAC-UF is superior to single UF and MXene-UF in terms of retention rate.

To evaluate the adsorption capacity of the membrane and both adsorbents during filtration, an adsorption test was conducted, as shown in Figure 5. Both MB and MO were

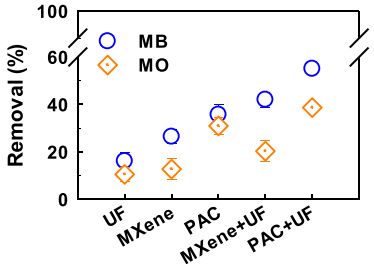

Figure 5. Adsorption of MB and MO on each adsorbent during filtration. Operating conditions: membrane area = 14.6 cm^2, adsorbent = 20 mg/L, dyes = 2 mg/L, pH = 7, conductivity = 100 μS/cm, and stirring speed = 200 rpm.

placed in contact with the membrane for 4 h and/or the adsorbents for 6 h. This contact time was selected to ensure the same contact time for single UF and both hybrid systems. The adsorption removal rate was on the order of PAC (35.7 and 30.9%) > MXene (26.7 and 12.4%) > membrane (16.1 and 10.5%) for MB and MO, respectively. The PAC and membrane adsorbed relatively similar amounts of both dyes, while the removal rate of MB with the MXene was higher than for MO. This is because electrostatic interaction plays an important role in the interaction between MXene and dyes. Therefore, these results confirm that, although MXene-UF exhibited a poorer retention performance than PAC-UF, as the retention rate between MB and MO is different, MXene-UF shows high selectivity due to electrostatic attraction or repulsion.

3.5. Effects of Different Solution Chemistry Conditions on Dye Retention in the MXene-UF. Based on the normalized permeate flux and retention rate results, the MXene-UF system has high potential to treat dyes, with a higher performance seen for MB than MO. Also, in general, some of the dye constituents, such as NOM, H^+/OH^-, and inorganic ions, coexist in real ecosystems. To fully explore the performance of MXene-UF for MB, the retention rate and normalized permeate flux were confirmed under a range of solution conditions. As shown in Figure 6a, the retention rate of MXene-UF increased with increasing HA concentration (51.7% for no HA, 58.5% for 2.5 mg/L, and 68.3% for 10 mg/L), while the normalized flux decreased with increasing HA concentration (0.96 for no HA, 0.91 for 2.5 m/L, and 0.79 for 10 mg/L). Also, all data in Figure 6a was not statistically the same average by a one-way complete statistical analysis of variance (ANOVA) test at a confidence level of 95%. These results presumably arise because the membrane active area was diminished by HA adsorption on the membrane. Due to the range of sizes of the HA (170−22 600 Da), pore plugging of the membrane (3000 Da) is possible.[46,47] In addition, aromatic components of HA can generate a fouling layer on the membrane surface through hydrophobic interaction,[48] and positively charged MB and the part of HA (which includes negatively charged carboxylic and phenolic groups at pH 7) can form complexes by electrostatic attraction as well as hydrophobic interaction, resulting in high retention and low permeate flux.[45]

The retention rate of MXene-UF at pH 3.5, 7, and 10.5 was 46.7, 51.7, and 57.7%, respectively, as shown in Figure 6b. The normalized flux for MXene-UF was observed to be 0.96, 0.96, and 0.95 at pH 3.5, 7, and 10.5, respectively. Although this result shows that the retention rate was similar regardless of solution pH by ANOVA results, a slightly higher retention rate was confirmed at pH 10.5. The MB might be adsorbed more on the MXene at higher pH due to the more abundant negative charged termination of MXene, as supported by the zeta potential result (Figure S1e).[49−51] In overall, the results (relatively high flux decline (Figure 2), high retention (Figure 4), high adsorption removal (Figure 5), and high retention with increasing pH (Figure 6) for MB compared to MO) indicate that electrostatic interaction was the most critical mechanism determining the MXene-UF performance.

Finally, the retention rate and normalized flux of MXene-UF for MB was evaluated with no ions, and with NaCl, $CaCl_2$, and Na_2SO_4, as shown in Figure 6c. Although ANOVA results indicate there are comparable retention results, the highest retention rate of 51.7% was observed with no ions (46.6% for NaCl, 43.4% for $CaCl_2$, and 47.7% for Na_2SO_4); similarly, the highest normalized flux of 0.96 was obtained with no ions (0.89 for NaCl, 0.84 for $CaCl_2$, and 0.90 for Na_2SO_4). In Section 3.4, it was shown that adsorption by MXene is the main cause of retention for MB in MXene-UF. However, the retention rate decreased with the addition of ions, because positive ions compete with MB for adsorption sites on the MXene via electrostatic attraction.[52] The normalized flux statistically evaluated at a confidence level of 95% by ANOVA also decreased in the presence of ions. This is likely because the presence of ions leads to a denser fouling layer and compacted membrane pores.[53,54] In addition, the formation of cross-linking between MXene and the membrane can affect the filtration system by the divalent cation bridging effect, leading to the lowest normalized flux with $CaCl_2$.[55]

4. CONCLUSIONS

$Ti_3C_2T_x$ MXene, as an adsorbent, was applied to a hybrid system based on adsorption combined with UF (MXene-UF) to treat selected dye compounds, including MB and MO. The normalized flux in MXene-UF (0.90 for MB and 0.92 for MO) exhibited better efficiency than a single UF system (0.86 for MB and 0.90 for MO), while another hybrid system, PAC-UF (0.72 for MB and 0.75 for MO), exhibited severe flux decline. This is because dyes can be adsorbed onto MXene, and only small quantities of MXene are deposited on the filtration membrane due to electrostatic repulsion. Both hybrid systems showed less irreversible fouling compared to single UF. A

https://dx.doi.org/10.1021/acsami.0c02454
ACS Appl. Mater. Interfaces 2020, 12, 16557−16565

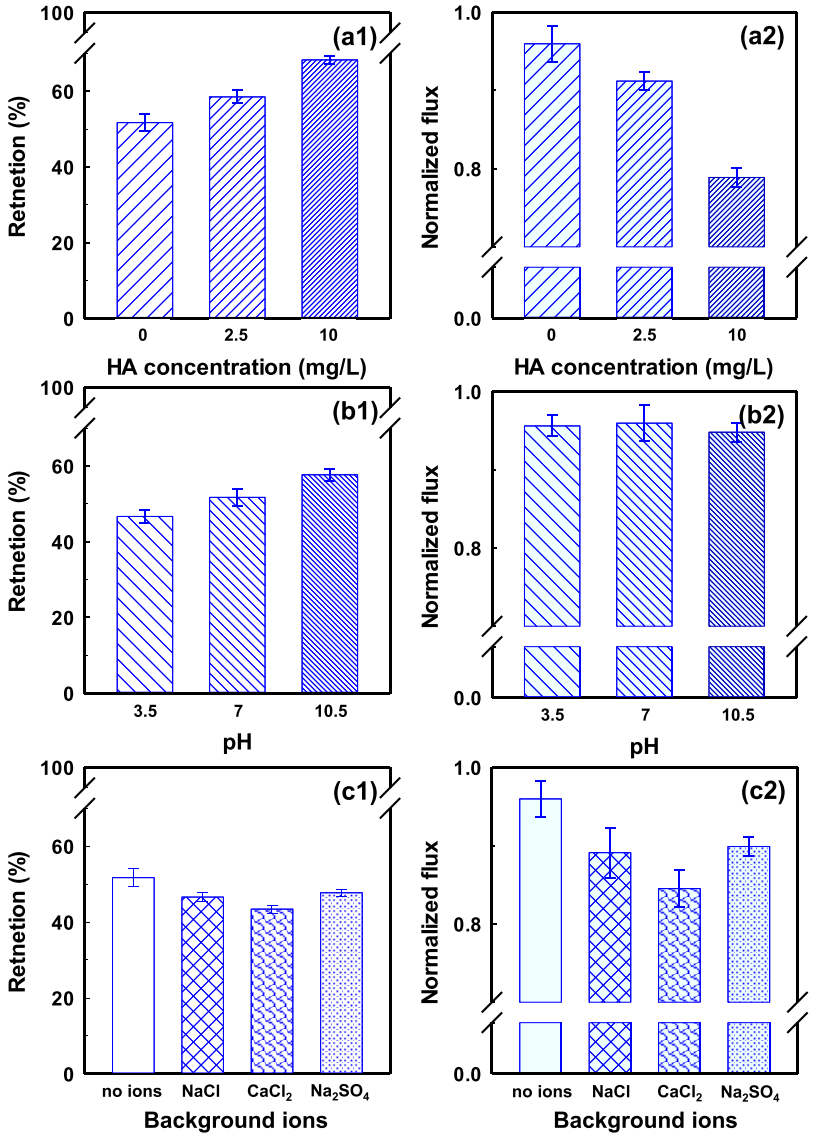

Figure 6. Retention and normalized flux under various (a) NOM concentrations, (b) pH conditions, and (c) background ions for MB in the MXene-UF system. Operating conditions: ΔP = 75 psi (520 kPa), adsorbent = 20 mg/L, MB = 2 mg/L, precontact time = 2 h, and stirring speed = 200 rpm.

resistance-in-series model, permeate flux modeling, and four conceptual blocking law models were used to investigate the behavior of the adsorbents, and it was observed that PAC acted as a strong foulant, resulting in severe fouling in PAC-UF. The average retention rates of PAC-UF (57.7 and 47.9%) were better than those for single UF (45.0 and 34.7%) and MXene-UF (51.7 and 34.9%) for MB and MO, respectively. This is because the membrane surface and pores can be more readily degraded by PAC adsorption on the membrane. PAC also has a higher surface area than MXene and hence can better adsorb the dyes. However, MXene-UF exhibited high selectivity, because electrostatic interaction is the main mechanism of dye treatment in the hybrid system. Taking into account the advantages of high permeate flux, lower irreversible fouling, and the high selectivity of MXene-UF, this is a promising advanced water treatment technology and a realistic alternative to conventional systems.

■ ASSOCIATED CONTENT

Supporting Information

The Supporting Information is available free of charge at https://pubs.acs.org/doi/10.1021/acsami.0c02454.

VCF, retention rate, and permeate flux equation (S1), characterization of MXene (Figure S1), zeta potential value of membrane (Figure S2), flux decline analysis (J^2 versus time and d^2t/dV^2 versus dt/dV) (Figure S3), flux decline analyses via d^2t/dV^2 versus dt/dV curves (Figure S4), physicochemical properties of selected dyes (Table S1), specifications of UF membrane (Table S2), composition of the synthetic dye wastewater (Table S3), and regression results of four conceptual blocking law models (Table S4) (PDF)

■ AUTHOR INFORMATION

Corresponding Author

Yeomin Yoon − *Department of Civil and Environmental Engineering, University of South Carolina, Columbia, South*

https://dx.doi.org/10.1021/acsami.0c02454
ACS Appl. Mater. Interfaces 2020, 12, 16557−16565

Carolina 29208, United States; orcid.org/0000-0001-9893-0924; Phone: 1-803-777-8952; Email: yoony@cec.sc.edu; Fax: 1-803-777-0670

Authors

Sewoon Kim − *Department of Civil and Environmental Engineering, University of South Carolina, Columbia, South Carolina 29208, United States*

Miao Yu − *Department of Chemical and Biological Engineering, Rensselaer Polytechnic Institute, Troy, New York 12180, United States;* orcid.org/0000-0003-4730-7563

Complete contact information is available at: https://pubs.acs.org/10.1021/acsami.0c02454

Notes

The authors declare no competing financial interest.

■ ACKNOWLEDGMENTS

This research was supported by the U.S. National Science Foundation (OIA-1632824).

■ REFERENCES

(1) Yu, S.; Wang, X.; Pang, H.; Zhang, R.; Song, W.; Fu, D.; Hayat, T.; Wang, X. Boron Nitride-Based Materials for the Removal of Pollutants from Aqueous Solutions: A Review. *Chem. Eng. J.* **2018**, *333*, 343−360.

(2) Sarker, M.; Shin, S.; Jeong, J. H.; Jhung, S. H. Mesoporous Metal-Organic Framework PCN-222 (Fe): Promising Adsorbent for Removal of Big Anionic and Cationic Dyes from Water. *Chem. Eng. J.* **2019**, *371*, 252−259.

(3) Sun, H.; Zhang, Y.; Sadam, H.; Ma, J.; Bai, Y.; Shen, X.; Kim, J.-K.; Shao, L. Novel Mussel-Inspired Zwitterionic Hydrophilic Polymer to Boost Mmembrane Water-Treatment Performance. *J. Membr. Sci.* **2019**, *582*, 1−8.

(4) Aftab, B.; Ok, Y. S.; Cho, J.; Hur, J. Targeted Removal of Organic Foulants in Landfill Leachate in Forward Osmosis System Integrated with Biochar/Activated Carbon Treatment. *Water Res.* **2019**, *160*, 217−227.

(5) Zhao, S.; Wang, Z. A Loose Nano-Filtration Membrane Prepared by Coating HPAN UF Membrane with Modified PEI for Dye Reuse and Desalination. *J. Membr. Sci.* **2017**, *524*, 214−224.

(6) Tahri, N.; Masmoudi, G.; Ellouze, E.; Jrad, A.; Drogui, P.; Amar, R. B. Coupling Microfiltration and Nanofiltration Processes for the Treatment at Source of Dyeing-Containing Effluent. *J. Cleaner Prod.* **2012**, *33*, 226−235.

(7) Schwarze, M.; Schaefer, L.; Chiappisi, L.; Gradzielski, M. Micellar Enhanced Ultrafiltration (MEUF) of Methylene Blue with Carboxylate Surfactants. *Sep. Purif. Technol.* **2018**, *199*, 20−26.

(8) Kim, S.; Park, C. M.; Jang, A.; Jang, M.; Hernández-Maldonado, A. J.; Yu, M.; Heo, J.; Yoon, Y. Removal of Selected Pharmaceuticals in an Ultrafiltration-Activated Biochar Hybrid System. *J. Membr. Sci.* **2019**, *570*, 77−84.

(9) Al-Bastaki, N.; Banat, F. Combining Ultrafiltration and Adsorption on Bentonite in a One-Step Process for the Treatment of Colored Waters. *Resour. Conserv. Recy.* **2004**, *41* (2), 103−113.

(10) Kim, J.; Cai, Z.; Benjamin, M. M. Effects of Adsorbents on Membrane Fouling by Natural Organic Matter. *J. Membr. Sci.* **2008**, *310* (1−2), 356−364.

(11) Lukatskaya, M. R.; Mashtalir, O.; Ren, C. E.; Dall'Agnese, Y.; Rozier, P.; Taberna, P. L.; Naguib, M.; Simon, P.; Barsoum, M. W.; Gogotsi, Y. Cation Intercalation and High Volumetric Capacitance of Two-Dimensional Titanium Carbide. *Science* **2013**, *341* (6153), 1502−1505.

(12) Jun, B.-M.; Kim, S.; Heo, J.; Park, C. M.; Her, N.; Jang, M.; Huang, Y.; Han, J.; Yoon, Y. Review of MXenes as New Nanomaterials for Energy Storage/Delivery and Selected Environmental Applications. *Nano Res.* **2019**, *12* (3), 471−487.

(13) Peng, J.; Chen, X.; Ong, W.-J.; Zhao, X.; Li, N. Surface and Heterointerface Engineering of 2D MXenes and Their Nanocomposites: Insights into Electro-and Photocatalysis. *Chem.* **2019**, *5* (1), 18−50.

(14) Wang, L.; Song, H.; Yuan, L.; Li, Z.; Zhang, P.; Gibson, J. K.; Zheng, L.; Wang, H.; Chai, Z.; Shi, W. Effective Removal of Anionic Re (VII) by Surface-Modified Ti_2CT_x MXene Nanocomposites: Implications for Tc (VII) Sequestration. *Environ. Sci. Technol.* **2019**, *53* (7), 3739−3747.

(15) Peng, Q.; Guo, J.; Zhang, Q.; Xiang, J.; Liu, B.; Zhou, A.; Liu, R.; Tian, Y. Unique Lead Adsorption Behavior of Activated Hydroxyl Group in Two-Dimensional Titanium Carbide. *J. Am. Chem. Soc.* **2014**, *136* (11), 4113−4116.

(16) Meng, F.; Seredych, M.; Chen, C.; Gura, V.; Mikhalovsky, S.; Sandeman, S.; Ingavle, G.; Ozulumba, T.; Miao, L.; Anasori, B.; et al. MXene Sorbents for Removal of Urea from Dialysate: A Step Toward the Wearable Artificial Kidney. *ACS Nano* **2018**, *12* (10), 10518−10528.

(17) Mashtalir, O.; Cook, K. M.; Mochalin, V.; Crowe, M.; Barsoum, M. W.; Gogotsi, Y. Dye Adsorption and Decomposition on Two-Dimensional Titanium Carbide in Aaqueous Media. *J. Mater. Chem. A* **2014**, *2* (35), 14334−14338.

(18) Westerhoff, P.; Yoon, Y.; Snyder, S.; Wert, E. Fate of Endocrine-Disruptor, Pharmaceutical, and Personal Care Product Chemicals During Simulated Drinking Water Treatment Processes. *Environ. Sci. Technol.* **2005**, *39* (17), 6649−6663.

(19) Kim, S.; Muñoz-Senmache, J. C.; Jun, B.-M.; Park, C. M.; Jang, A.; Yu, M.; Hernández-Maldonado, A. J.; Yoon, Y. A Metal Organic Framework-Ultrafiltration Hybrid System for Removing Selected Pharmaceuticals and Natural Organic Matter. *Chem. Eng. J.* **2020**, *382*, 122920.

(20) Mulder, M. *Basic principles of membrane technology*, 2nd ed.; Springer Science & Business Media, 1996.

(21) Dhakal, N.; Salinas-Rodriguez, S. G.; Ouda, A.; Schippers, J. C.; Kennedy, M. D. Fouling of Ultrafiltration Membranes by Organic Matter Generated by Marine Algal Species. *J. Membr. Sci.* **2018**, *555*, 418−428.

(22) Danis, U.; Aydiner, C. Investigation of Process Performance and Fouling Mechanisms in Micellar-Enhanced Ultrafiltration of Nickel-Contaminated Waters. *J. Hazard. Mater.* **2009**, *162* (2−3), 577−587.

(23) Hermia, J. Constant Pressure Blocking Filtration Laws-Application to Power-Law Non-Newtonian Fluids. *Trans. Inst. Chem. Eng.* **1982**, *60*, 183−187.

(24) Aslam, M.; Lee, P.-H.; Kim, J. Analysis of Membrane Fouling with Porous Membrane Filters by Microbial Suspensions for Autotrophic Nitrogen Transformations. *Sep. Purif. Technol.* **2015**, *146*, 284−293.

(25) Naguib, M.; Mochalin, V. N.; Barsoum, M. W.; Gogotsi, Y. 25th anniversary article: MXenes: A New Family of Two-Dimensional Materials. *Adv. Mater.* **2014**, *26* (7), 992−1005.

(26) Wei, Z.; Peigen, Z.; Wubian, T.; Xia, Q.; Yamei, Z.; ZhengMing, S. Alkali Treated $Ti_3C_2T_x$ MXenes and Their Dye Adsorption Performance. *Mater. Chem. Phys.* **2018**, *206*, 270−276.

(27) Tariq, A.; Ali, S. I.; Akinwande, D.; Rizwan, S. Efficient Visible-Light Photocatalysis of 2D-MXene Nanohybrids with Gd^{3+} and Sn^{4+} Codoped Bismuth Ferrite. *ACS Omega* **2018**, *3* (10), 13828−13836.

(28) Fard, A. K.; Mckay, G.; Chamoun, R.; Rhadfi, T.; Preud'Homme, H.; Atieh, M. A. Barium Removal from Synthetic Natural and Produced Water Using MXene as Two Dimensional (2-D) Nanosheet Adsorbent. *Chem. Eng. J.* **2017**, *317*, 331−342.

(29) Ma, X.; Chen, P.; Zhou, M.; Zhong, Z.; Zhang, F.; Xing, W. Tight Ultrafiltration Ceramic Membrane for Separation of Dyes and Mixed Salts (both $NaCl/Na_2SO_4$) in Textile Wastewater Treatment. *Ind. Eng. Chem. Res.* **2017**, *56* (24), 7070−7079.

(30) An, A. K.; Guo, J.; Jeong, S.; Lee, E.-J.; Tabatabai, S. A. A.; Leiknes, T. High Flux and Antifouling Properties of Negatively Charged Membrane for Dyeing Wastewater Treatment by Membrane Distillation. *Water Res.* **2016**, *103*, 362−371.

(31) Zhang, N.; Chen, S.; Yang, B.; Huo, J.; Zhang, X.; Bao, J.; Ruan, X.; He, G. Effect of Hydrogen-Bonding Interaction on the Arrangement and Dynamics of Water Confined in a Polyamide Membrane: A molecular Dynamics Simulation. *J. Phys. Chem. B* **2018**, *122* (17), 4719−4728.
(32) Xu, G.-R.; Wang, J.-N.; Li, C.-J. Strategies for Improving the Performance of the Polyamide Thin Film Composite (PA-TFC) Reverse Osmosis (RO) Membranes: Surface Modifications and Nanoparticles Incorporations. *Desalination* **2013**, *328*, 83−100.
(33) Löwenberg, J.; Zenker, A.; Baggenstos, M.; Koch, G.; Kazner, C.; Wintgens, T. Comparison of Two PAC/UF Processes for the Removal of Micropollutants from Wastewater Treatment Plant Effluent: Process Performance and Removal Efficiency. *Water Res.* **2014**, *56*, 26−36.
(34) Susanto, H.; Ulbricht, M. High-Performance Thin-Layer Hydrogel Composite Membranes for Ultrafiltration of Natural Organic Matter. *Water Res.* **2008**, *42* (10−11), 2827−2835.
(35) Aoustin, E.; Schäfer, A.; Fane, A. G.; Waite, T. Ultrafiltration of Natural Organic Matter. *Sep. Purif. Technol.* **2001**, *22-23*, 63−78.
(36) Jucker, C.; Clark, M. M. Adsorption of Aquatic Humic Substances on Hydrophobic Ultrafiltration Membranes. *J. Membr. Sci.* **1994**, *97*, 37−52.
(37) Chu, K. H.; Huang, Y.; Yu, M.; Her, N.; Flora, J. R.; Park, C. M.; Kim, S.; Cho, J.; Yoon, Y. Evaluation of Hhumic Acid and Tannic Acid Fouling in Graphene Oxide-Coated Ultrafiltration Membranes. *ACS Appl. Mater. Interfaces* **2016**, *8* (34), 22270−22279.
(38) Ju, Y.; Hong, I.; Hong, S. Multiple MFI Measurements for the Evaluation of Organic Fouling in SWRO Desalination. *Desalination* **2015**, *365*, 136−143.
(39) Boerlage, S. F.; Kennedy, M. D.; Dickson, M. R.; El-Hodali, D. E.; Schippers, J. C. The Modified Fouling Index Using Ultrafiltration Membranes (MFI-UF): Characterisation, Filtration Mechanisms and Proposed Reference Membrane. *J. Membr. Sci.* **2002**, *197* (1−2), 1−21.
(40) Kirschner, A. Y.; Cheng, Y.-H.; Paul, D. R.; Field, R. W.; Freeman, B. D. Fouling Mechanisms in Constant Flux Crossflow Ultrafiltration. *J. Membr. Sci.* **2019**, *574*, 65−75.
(41) Ma, J.; Yu, F.; Zhou, L.; Jin, L.; Yang, M.; Luan, J.; Tang, Y.; Fan, H.; Yuan, Z.; Chen, J. Enhanced Adsorptive Removal of Methyl Orange and Methylene Blue from Aqueous Solution by Alkali-Activated Multiwalled Carbon Nanotubes. *ACS Appl. Mater. Interfaces* **2012**, *4* (11), 5749−5760.
(42) Liu, B.; Qu, F.; Liang, H.; Van der Bruggen, B.; Cheng, X.; Yu, H.; Xu, G.; Li, G. Microcystis aeruginosa-laden surface water treatment using ultrafiltration: Membrane fouling, cell integrity and extracellular organic matter rejection. *Water Res.* **2017**, *112*, 83−92.
(43) Falca, G.; Musteata, V.-E.; Behzad, A. R.; Chisca, S.; Nunes, S. P. Cellulose Hollow Fibers for Organic Resistant Nanofiltration. *J. Membr. Sci.* **2019**, *586*, 151−161.
(44) Lin, K.-Y. A.; Chang, H.-A. Ultra-High Adsorption Capacity of Zeolitic Imidazole Framework-67 (ZIF-67) for Removal of Malachite Green from Water. *Chemosphere* **2015**, *139*, 624−631.
(45) Lin, J.; Ye, W.; Baltaru, M.-C.; Tang, Y. P.; Bernstein, N. J.; Gao, P.; Balta, S.; Vlad, M.; Volodin, A.; Sotto, A.; et al. Tight Ultrafiltration Membranes for Enhanced Separation of Dyes and Na_2SO_4 during Textile Wastewater Treatment. *J. Membr. Sci.* **2016**, *514*, 217−228.
(46) Sun, J.; Hu, C.; Tong, T.; Zhao, K.; Qu, J.; Liu, H.; Elimelech, M. Performance and Mechanisms of Ultrafiltration Membrane Fouling Mitigation by Coupling Coagulation and Applied Electric Field in a Novel Electrocoagulation Membrane Reactor. *Environ. Sci. Technol.* **2017**, *51* (15), 8544−8551.
(47) Tang, C. Y.; Kwon, Y.-N.; Leckie, J. O. Characterization of Humic Acid Fouled Reverse Osmosis and Nanofiltration Membranes by Transmission Electron Microscopy and Streaming Potential Measurements. *Environ. Sci. Technol.* **2007**, *41* (3), 942−949.
(48) Nghiem, L. D.; Vogel, D.; Khan, S. Characterising Humic Acid Fouling of Nanofiltration Membranes Using Bisphenol A as a Molecular Indicator. *Water Res.* **2008**, *42* (15), 4049−4058.
(49) Liu, G.; Zou, J.; Tang, Q.; Yang, X.; Zhang, Y.; Zhang, Q.; Huang, W.; Chen, P.; Shao, J.; Dong, X. Surface Modified Ti_3C_2 MXene Nanosheets for Tumor Targeting Photothermal/Photodynamic/Chemo Synergistic Therapy. *ACS Appl. Mater. Interfaces* **2017**, *9* (46), 40077−40086.
(50) Ying, Y.; Liu, Y.; Wang, X.; Mao, Y.; Cao, W.; Hu, P.; Peng, X. Two-Dimensional Titanium Carbide for Efficiently Reductive Removal of Highly Toxic Chromium (VI) from Water. *ACS Appl. Mater. Interfaces* **2015**, *7* (3), 1795−1803.
(51) Deng, H.; Yang, L.; Tao, G.; Dai, J. Preparation and Characterization of Activated Carbon from Cotton Stalk by Microwave Assisted Chemical Activation—Application in Methylene Blue Adsorption from Aqueous Solution. *J. Hazard. Mater.* **2009**, *166* (2−3), 1514−1521.
(52) Jiang, C.; Garg, S.; Waite, T. D. Iron Redox Transformations in the Presence of Natural Organic Matter: Effect of Calcium. *Environ. Sci. Technol.* **2017**, *51* (18), 10413−10422.
(53) Shankar, V.; Heo, J.; Al-Hamadani, Y. A.; Park, C. M.; Chu, K. H.; Yoon, Y. Evaluation of Biochar-Ultrafiltration Membrane Processes for Humic Acid Removal Under Various Hydrodynamic, pH, Ionic Strength, and Pressure Conditions. *J. Environ. Manage.* **2017**, *197*, 610−618.
(54) Visvanathan, C.; Marsono, B. D.; Basu, B. Removal of THMP by Nanofiltration: Effects of Interference Parameters. *Water Res.* **1998**, *32* (12), 3527−3538.
(55) Yin, Z.; Wen, T.; Li, Y.; Li, A.; Long, C. Pre-Ozonation for the Mitigation of Reverse Osmosis (RO) Membrane Fouling by Biopolymer: The roles of Ca^{2+} and Mg^{2+}. *Water Res.* **2020**, *171*, 115437.

https://dx.doi.org/10.1021/acsami.0c02454
ACS Appl. Mater. Interfaces 2020, 12, 16557−16565